Signal dependence and noise source in ultrasound-modulated optical tomography

Gang Yao and Lihong V. Wang

A Monte Carlo modeling technique was used to simulate ultrasound-modulated optical tomography in inhomogeneous scattering media. The contributions from two different modulation mechanisms were included in the simulation. Results indicate that ultrasound-modulated optical signals are much more sensitive to small embedded objects than unmodulated intensity signals. The differences between embedded absorption and scattering objects in the ultrasound-modulated optical signals were compared. The effects of neighboring inhomogeneity and background optical properties on the ultrasound-modulated optical signals were also studied. We analyzed the signal-to-noise ratio in the experiment and found that the major noise source is the speckle noise caused by small particle movement within the biological tissue sample. We studied this effect by incorporating a Brownian motion factor in the simulation.

OCIS codes: 170.3880, 120.6150, 110.7050, 110.7170.

1. Introduction

Because of its noninvasive, nonionization properties, optical imaging of biological tissues has been an active research area in recent years.[1,2] A number of different optical imaging techniques have been proposed and studied, such as time-resolved optical imaging, frequency-domain optical imaging, and optical coherence tomography. The contrast of optical imaging is primarily generated by the optical absorption properties and the scattering properties of living tissue. Because biological tissues are highly scattering media, deep-tissue optical imaging usually employs sophisticated reconstruction algorithms to achieve a good imaging depth and reasonable resolution. In addition to the purely optical imaging techniques, combinations of optical techniques with ultrasonic techniques have also been explored, including optoacoustic imaging,[3–5] sonoluminescence tomography,[6] and ultrasound-modulated optical tomography.[7–14] In these hybrid methods, ultrasonic waves were used to furnish localization information because they are much less scattering in biological tissues.

In ultrasound-modulated optical tomography, some light is modulated by an ultrasonic wave inside the biological tissue to carry ultrasonic frequency. Such tagged photons can be discriminated from the background unmodulated photons by signal processing, and their originations are directly related to the position of the ultrasonic column inside the tissue. Marks *et al.*[7] first investigated the possibility of probing breast cancer using this technique. Wang *et al.*[8,9] developed ultrasound-modulated optical tomography and obtained images in tissue-simulating phantoms. Since then, many new technologies such as parallel speckle detection by Leveque *et al.*,[11] frequency-swept ultrasound-modulated optical tomography by Wang and Ku,[13] speckle-contrast detection by Li *et al.*,[15] and other technologies[16,17] have been developed. To understand the mechanisms involved in acousto-optic interactions in scattering media, Wang[18] developed a theoretical model that considered two important phase modulation mechanisms: the refractive-index modulation and particle displacements. The analytical results agreed well with a Monte Carlo simulation[19] for ultrasound modulation of a volumetric homogeneous scattering medium. Sakadzic and Wang[20] further extended the model to include anisotropic scattering media.

For imaging applications, however, ultrasonic transducers with small focal size are used to achieve spatial resolution. In addition, the inho-

G. Yao is with the Department of Biological Engineering, University of Missouri-Columbia, Columbia, Missouri 65211. L. V. Wang (lwang@tamu.edu) is with the Optical Imaging Laboratory, Department of Biomedical Engineering, Texas A&M University, College Station, Texas 77843-3120.

Received 20 August 2003; revised manuscript received 17 November 2003; accepted 21 November 2003.

0003-6935/04/061320-07$15.00/0

mogeneous nature of turbid media adds complexity to the signal interpretation in ultrasound-modulated optical tomography. These effects cannot be studied by the analytical models used for volumetric modulation.[18–20] In this study, a Monte Carlo technique was used to simulate the sensitivity and the contrast of this technique. The two modulation mechanisms, i.e., refractive-index modulation and particle displacement, were incorporated in the simulation. We also studied the effects of speckle noise caused by Brownian motion, which is the most important noise in experiments involving biological tissue.

2. Method

In ultrasound-modulated optical tomography, the transmitted light consists of two parts: the ac photons that are modulated by the ultrasonic wave and the dc background photons that are not modulated. Only those photons passing through the ultrasonic column can be modulated. The modulated depth (ac and dc) reflects the local optical and ultrasonic properties within the ultrasonic beam and can be used for tomographic imaging of the scattering medium.

The intensity of transmitted light can be written as (Wiener–Khinchin theorem)

$$I_n = \frac{1}{T_a}\int_0^{T_a} \cos(n\omega_a\tau)G_1(\tau)\mathrm{d}\tau, \tag{1}$$

where T_a is the period of ultrasonic oscillation, ω_a is the ultrasonic frequency, and $G_1(\tau)$ is the autocorrelation function of the scattered light:

$$G_1(\tau) = \int_0^{\infty} p(s)\langle E_s(t)E_s(t+\tau)\rangle_t \mathrm{d}s, \tag{2}$$

where $p(s)$ is the probability density function of path length s and E_s is the electrical field of the light scattered along path s. The correlation function is calculated from the contributions from random Brownian (B) motion and ultrasonic (U) modulation[21],

$$\langle E_s(t)E_s(t+\tau)\rangle = \langle E_s(t)E_s(t+\tau)\rangle_B\langle E_s(t)E_s(t+\tau)\rangle_U. \tag{3}$$

The contribution from Brownian motion is determined by the particle relaxation time τ_0, the mean free path l, and the total path length s:

$$\langle E_s(t)E_s(t+\tau)\rangle_B = \exp\left(-\frac{2s}{\tau_0 l}\tau\right). \tag{4}$$

We can calculate the contribution from ultrasonic modulation by accumulating the optical phase variations induced by ultrasound,

$$\langle E_s(t)E_s(t+\tau)\rangle_U = \langle \exp[-i(\Delta\Phi_n + \Delta\Phi_d)]\rangle, \tag{5}$$

where $\Delta\Phi_n$ is the total phase variation caused by refractive-index modulation of the scattering medium and $\Delta\Phi_d$ is the total phase variation caused by displacement of the scattering particles. The equations to calculate these phase variations have been given in detail by Wang.[18,19] The modulation depth at ultrasonic frequency can be calculated as $M = I_1/I_0$ from Eq. (1).

A Monte Carlo method was used to simulate light transport in scattering media. The basic simulation procedures have been described in detail elsewhere.[19] The program was extended to handle multiple objects to simulate the effects of a heterogeneous background. In the simulation, the tissue sample was modeled as a slab containing embedded objects. For simplicity, the object and the ultrasonic column were modeled as cylinders with certain heights. The photon packet was launched perpendicularly into the tissue. Geometric calculations were performed to determine if the path of a photon packet crossed one of the objects. We sampled the scattering angles of a photon packet using optical properties. The phase variation of a photon packet was accumulated whenever the photon intersected with the ultrasound column or was scattered within the ultrasound column. We calculated the correlation function of the transmitted light by accumulating contributions from all transmitted photons.

Unless indicated specifically, the following optical properties of the background scattering media were used in the simulation[22]: the refractive index $n = 1.33$, the absorption coefficient $\mu_a = 0.1\ \mathrm{cm}^{-1}$, the scattering coefficient $\mu_s = 20.0\ \mathrm{cm}^{-1}$, and the anisotropy factor $g = 0.9$. The thickness of the tissue slab is 3 cm. Both the object and the ultrasonic column have a radius of 1 mm and a height of 10 mm, although their dimensions are not required to be identical in the simulations. The velocity of the ultrasonic wave is 1480 m/s. The ultrasound amplitude is 0.1 nm. The ultrasound wave vector is $4 \times 10^3\ \mathrm{m}^{-1}$ that corresponds to a wavelength of 1.57 mm in the scattering media. A light beam with a radius of 1 cm is incident perpendicularly upon the turbid medium. Only the transmitted photons within a circular disk with a 1-cm radius on the exit plane, simulating the detection area, were scored.

3. Results

A. Sensitivity to Optical Properties

In ultrasound-modulated optical tomography, the modulated photons carry the optical as well as the ultrasonic properties of the ultrasonic column. If the optical properties within the ultrasonic column are different, the detected signal will be different. Ultrasonic heterogeneity and Brownian motion were not considered in this simulation. To study the effects of these different optical properties, we simulated objects with different absorption coefficients and scattering coefficients. The simulation results are shown in Fig. 1. A single cylindrical object is buried at the center of the tissue slab. The position of the ultrasonic column is aligned with the object [Fig. 1(a)]. Therefore every photon passing through the object will be labeled by the ultrasound. The

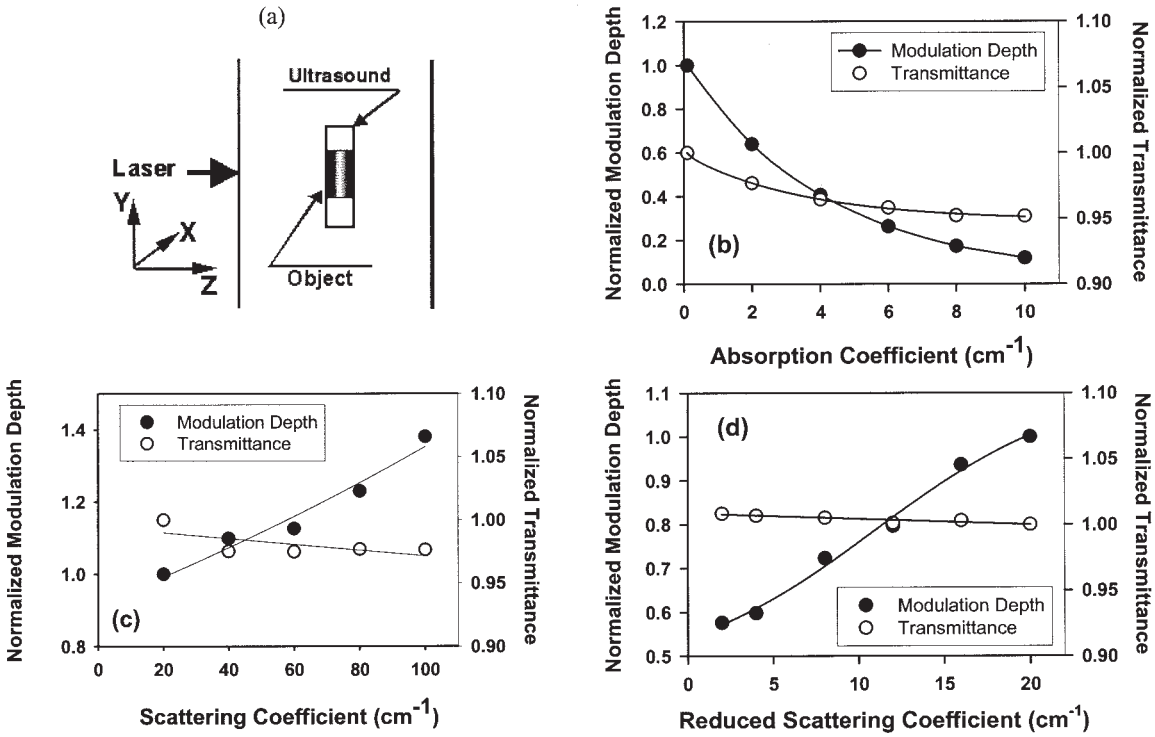

Fig. 1. (a) Configuration of the scattering medium and the ultrasound. Modulation depth and total transmittance versus the (b) absorption coefficient, (c) scattering coefficient, and (d) reduced scattering coefficient.

values in the plots in Figs. 1(b)–1(d) are normalized to the signal values obtained when the embedded object has the same optical properties of the background medium.

From the simulation results, the modulation signal is much more sensitive to the change of optical properties than the total output intensity (transmittance). For example, as the optical absorption coefficient of the object increases 100 times, the modulation depth decreases by ~88%, whereas the transmittance only decreases by ~5%. The modulation depth decreases as the absorption coefficient of the object increases because more photons passing through the object have been absorbed. If only the absorption coefficient μ_a of the object is the changed by $\Delta\mu_a$, the modulation signal changes by

$$\Delta M \propto -\int M(p)\exp(-\Delta\mu_a p) f(p)\mathrm{d}p, \qquad (6)$$

where $M(p)$ is the intensity of modulated photons having path length p inside the object before the absorption coefficient is varied and $f(p)$ is the distribution of p. If $\Delta\mu_a p$ is much less than unity, the Δac will be linearly proportional to $\Delta\mu_a$. When the absorption coefficient is changed by 100-fold from 0.1 to 10 cm^{-1}, the modulated photons of p values that are comparable with the 0.2-cm diameter of the embedded object will vary by a factor of $\exp(-9.9 \times 0.2) = 14\%$, which roughly matches the simulated ~88% decrease.

The scattering properties (μ_s and g) of the embedded object have even less of an effect on the total transmittance than the absorption property (μ_a). However, the modulation depth still shows significant sensitivities for these changes. In the example, when the scattering increases from 20 to 100 cm^{-1}, the modulation depth increases by ~40% whereas the total transmission decreases only by less than 3%. If the scattering properties of the object are changed, the paths of the photons will be altered. Although a simple expression similar to relation (6) does not exist, the increase of the scattering coefficient of the embedded object causes the photons to have more scattering events and longer path lengths within the ultrasound column. Both effects will lead to a higher modulation depth. Figure 1(d) shows that the modulation depth decreases as the anisotropic factor of the embedded object increases. In Fig. 1(d), the scattering coefficient of the object was fixed at 20 cm^{-1} in the simulation. Calculation indicated that the average path length inside the ultrasound column is higher at a smaller anisotropic factor, which leads to a higher modulation depth because of the refractive-index modulation mechanism.

Figure 2 shows the results of modulation depth and transmittance when the absorbing object is not aligned with the source–detector axis. The modulation depth decreases slightly as the object moves away from the central axis. This is caused by the inhomogeneous distribution of light inside the sample.[12] However, the fractional change as plotted in Fig. 1 has little change. In addition, there is no significant change in the transmittance. Therefore

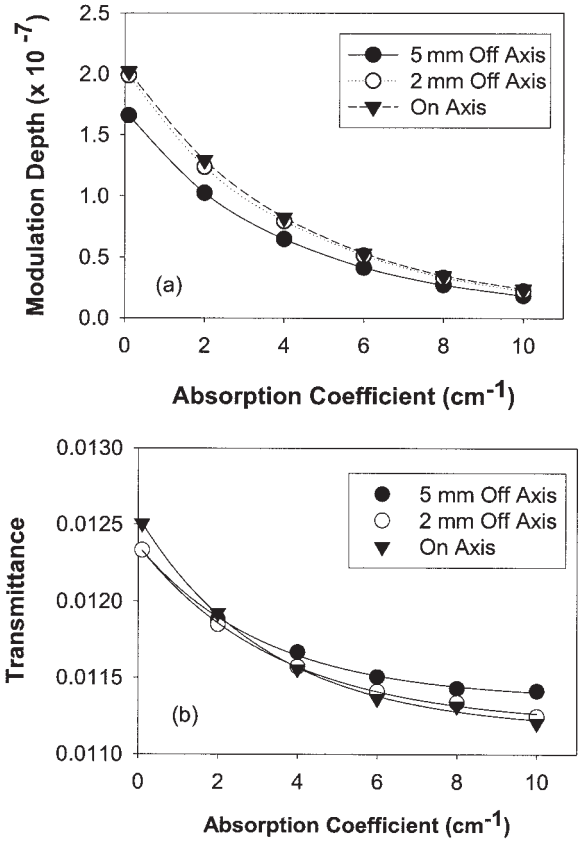

Fig. 2. Comparison of the calculated results of (a) the modulation depth and (b) transmittance when the object center is shifted from the system optical axis along the x axis.

the modulated signal is still much more sensitive than the nonmodulated transmittance even if the object is not aligned with the source–detector axis.

B. Effect of Inhomogeneity

In ultrasound-modulated optical tomography, we can usually obtain two-dimensional images by mechanically scanning the ultrasonic transducer over the sample. A measured modulation depth is directly assigned as the signal intensity at the corresponding ultrasound location. Because the local modulated signal intensity depends on the local optical fluence, the internal optical fluence affects the obtained images. Because the light fluence distribution is not uniform within the scattering medium, the modulation depth is related to the position of the ultrasonic column even in a homogeneous medium.[12]

In reality, tissue samples are inhomogeneous in both absorption and scattering properties. A buried object will affect the optical fluence in its neighborhood and the modulated signal intensity. Figure 3(a) shows such an example in which two identical objects are separated by 3 mm along the z axis. The ultrasonic column is located at object 1, which is at the center of the slab. Brownian motion is not considered in the simulation. From the results [Figs. 3(b) and 3(c)], the calculated modulation depth is affected by the optical properties of the other neighboring object. As the absorption coefficient and the scattering coefficient of object 2 increase, the signal values of object 1 decrease because the modulated light decreases after passing through object 2. In other words, object 2 casts a shadow on object 1 when an image of the scattering medium is produced. Such cross talks depend on the optical properties, the distance, and the size of neighboring objects.

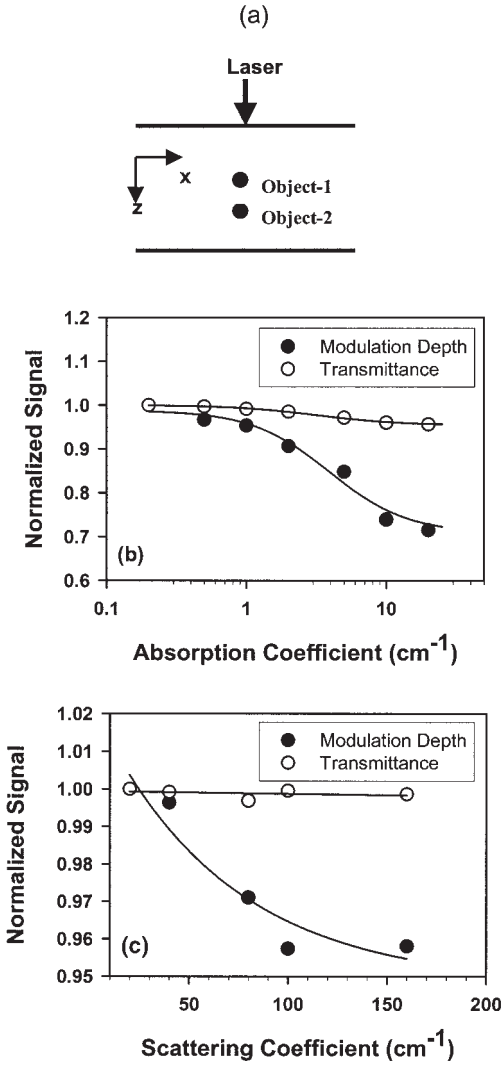

Fig. 3. (a) Configuration of the two embedded objects in the simulation of the effects of neighboring objects. The two objects are separated by 3 mm along the z axis. Modulation depth and total transmittance versus the (b) absorption coefficient and (c) scattering coefficient of the second object.

The absolute signal level is also affected by the optical properties of the background medium. In Fig. 4(a), the modulation signal of a single object was calculated with different background scattering coefficients. The object was positioned at the center of the turbid medium. Its optical properties are $\mu_a = 2$ cm^{-1}, $\mu_s = 100.0$ cm^{-1}, and $g = 0.9$. It is interesting to see that modulation depth increases as the background scattering coefficient increases because more photons interact with the ultrasonic column. Both

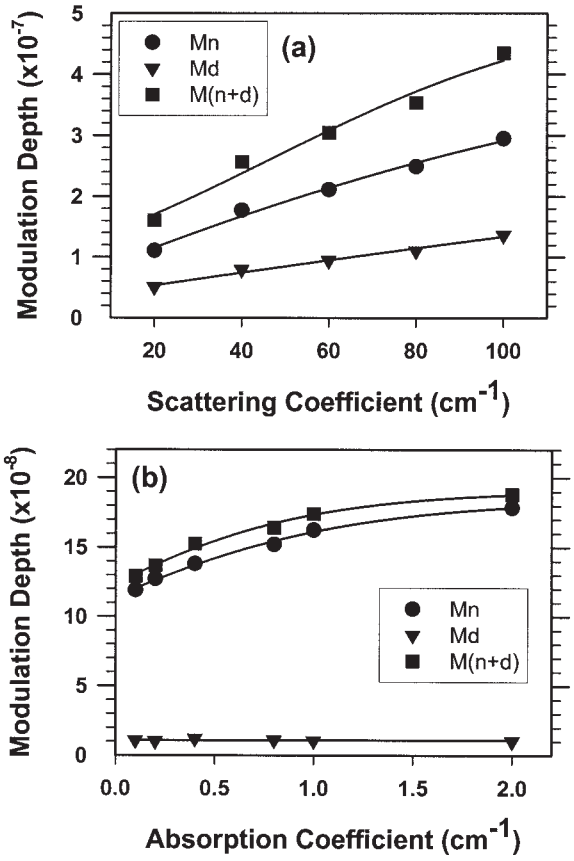

Fig. 4. Modulation depth and total transmittance versus the background (a) scattering coefficient and (b) absorption coefficient. $M(n)$, refractive-index modulation; $M(d)$, particle displacement modulation; $M(n + d)$, modulation by both mechanisms.

modulation mechanisms contribute to this effect. Detailed calculations show that both the average scattering events of the modulated photons and their path lengths within the ultrasound column increase as the background scattering coefficient increases, which explains the above observation. Figure 4(b) shows the effect of the background absorption coefficient. The object's optical properties are $\mu_a = 2$ cm^{-1}, $\mu_s = 20.0$ cm^{-1}, and $g = 0.9$. The modulation depth increases slightly as the background absorption coefficient increases because more unmodulated photons are absorbed. The increase is mainly due to the modulation of the refractive index.

The above examples indicate that the signal intensity is indeed related to the background properties and object distribution in the scattering medium. Therefore quantitative measurements of the optical properties of the embedded objects entail sophisticated reconstruction algorithms.

C. Noise and Speckle

In ultrasound-modulated optical tomography, the signal-to-noise ratio is critical because the modulated signal is very small. To improve experimental results, system noise properties should be carefully analyzed and optimized. There are many possible noise sources in the experimental system including contributions from both the optical system and the ultrasonic system. Among all the noise sources, the shot noise is the theoretical limit of noise, and the speckle noise appears to be the most significant noise source in biological tissue. Speckle noise is caused by the random movement of small particles within the biological tissue. These particle movements change the speckle patterns and induce noise in the detected optical signals.

To demonstrate speckle noise, we examined the system performance using ground glass as the sample without ultrasound modulation. A laser beam (Melles-Griot, 56IMS667) illuminated the ground glass, and the generated speckle pattern was recorded by a CCD camera (DALSA CA-D1-0256T). A total of 200 frames of such speckle images was recorded in ~3.2 s. The standard deviation of each pixel in the CCD image was calculated and subsequently normalized to the shot noise obtained by the square root of the average digital count in the pixel. As shown in Fig. 5(a), the measured noise level was within two times of the shot noise when ground glass was used and the light path was in the air. In other words, it can be assumed that the whole experimental system was operating quite closely to the shot-noise-limited level.

However, the noise level increased to more than five times the shot noise when a water tank was inserted into the light path between the ground glass and the CCD [Fig. 5(b)]. This was caused by fluctuations of the water and the movement of small particles in the water, which disturbed the speckle pattern. The noise level further increased to more than ten times the shot noise when chicken breast tissue was used instead of the ground glass [Fig. 5(c)]. One reason is that chicken breast tissue is a volume scattering medium in which light has a longer path length. The movements of small particles within the tissue disturb the speckle patterns. It is clear that this dynamic speckle change is the major noise source in the experiments. Increasing the exposure time reduces the speckle fluctuation. Unfortunately, this effect is equivalent to speckle averaging and therefore reduces the modulation depth. A better method is to acquire the signal within the speckle correlation time. The correlation time can be measured in the experiments when multiple frames of the images are continuously acquired. A typical measurement of ex vivo chicken breast tissue is shown in Fig. 6, in which the correlation time was approximately 100 ms.

The speckle correlation time is related to the particle relaxation time in the scattering medium. With a small relaxation time, particles move fast and cause a short speckle correlation time. We simulated the effect of random movement of small particles by incorporating Brownian motion [Eq. (4)] into the Monte Carlo simulation. Photons that are not interacting with ultrasound are dominant in this effect because their amount is much larger than modulated photons. Figure 7 shows an example of

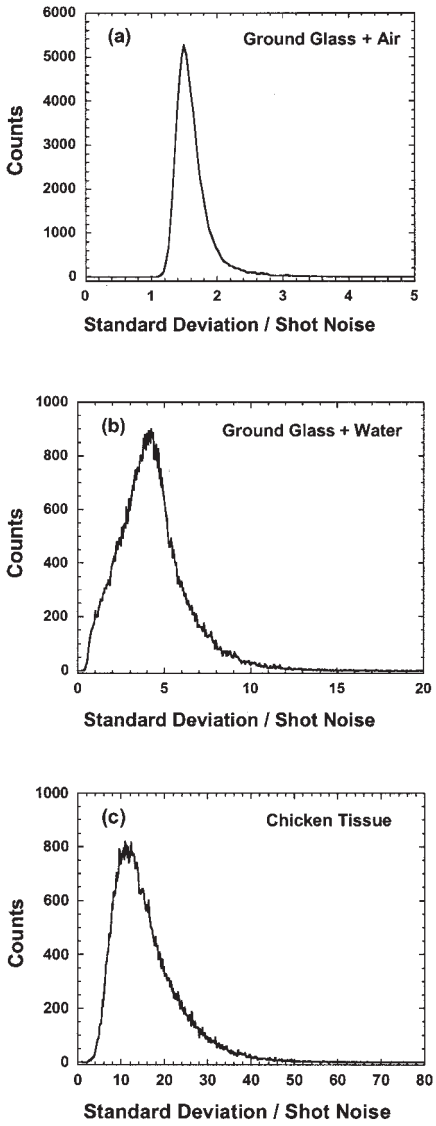

Fig. 5. Speckle pattern stability with different samples.

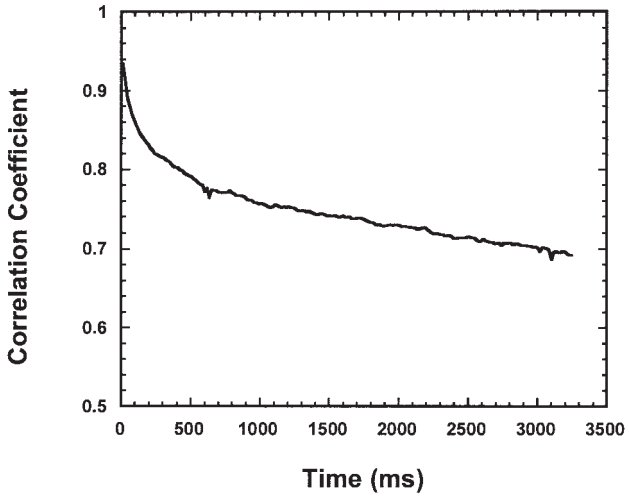

Fig. 6. Speckle correlation measured from 1.2-cm-thick chicken breast.

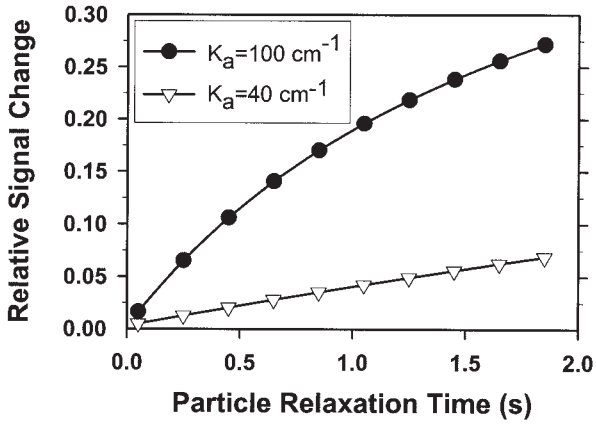

Fig. 7. Effect of particle relaxation time on signal sensitivity.

signal sensitivity dependency on the particle relaxation time. Two small absorption objects were used in the simulation. Their absorption coefficients are 0.2 and 2.0 cm^{-1} respectively. The y axis in Fig. 7 is plotted as the relative modulation depth that is defined as $[M(\mu_a = 2.0) - M(\mu_a = 0.2)]/M(\mu_a = 0.2)$. At small particle relaxation time, the modulation depths obtained at these two objects are indistinguishable. The signal difference becomes larger as the relaxation time increases. The results also show that modulation depth at a higher ultrasonic frequency has better sensitivity than that at a lower ultrasonic frequency. This is because the autocorrelation signal is calculated within one ultrasonic period, which is smaller at high frequency. This result implies that the speckle decorrelation problem may have less of an effect when high-frequency ultrasound is applied.

4. Conclusions

A Monte Carlo simulation was applied to study the signal sensitivity of ultrasound-modulated optical tomography. The simulation study indicates that this technology is significantly more sensitive to small optical objects than unmodulated intensity measurements. In addition, an inhomogeneous tissue background will alter the signal intensity. Therefore obtaining accurate optical properties by simple direct imaging scanning requires use of sophisticated reconstruction.

Optical speckles play an extremely important role in the experiments. Time variation of speckle patterns represents the largest source of noise in an experiment, especially if the biological tissue is thick. To overcome this problem, data must be acquired within the speckle correlation time. Our study also indicated that ultrasound modulation with higher frequency has better immunization to speckle variations.

This project was sponsored by a Summer Faculty Research Fellowship (for G. Yao) from the University of Missouri-Columbia and in part (for L. V. Wang) by National Institutes of Health grant R01 CA71980,

National Science Foundation grant BES-9734491, and Texas Higher Education Coordinating Board grant 000512-0063-2001.

References

1. R. R. Alfano and J. G. Fujimoto, eds., *Advances in Optical Imaging and Photon Migration*, Vol. 2 of OSA Trends in Optics and Photonics Series (Optical Society of America, Washington, D.C., 1996).
2. B. Chance and R. R. Alfano, eds., *Optical Tomography and Spectroscopy of Tissue: Theory, Instrumentation, Model, and Human Studies II*, Proc. SPIE **2979** (1997).
3. R. A. Kruger and P. Liu, "Photoacoustic ultrasound: theory," in *Laser-Tissue Interaction V*, S. L. Jacques, ed., Proc. SPIE **2134A,** 114–118 (1994).
4. A. A. Oraevsky, R. O. Esenaliev, S. L. Jacques, and F. K. Tittel, "Laser optic-acoustic tomography for medical diagnostics: principles," in *Biomedical Sensing, Imaging, and Tracking Technologies I*, R. A. Lieberman, H. Podbielska, and T. Vo-Dinh, eds., Proc. SPIE **2676,** 22–31 (1996).
5. C. G. A. Hoelen, F. F. M. De Mul, R. Pongers, and A. Dekker, "Three-dimensional photoacoustic imaging of blood vessels in tissue," Opt. Lett. **23,** 648–650 (1998).
6. L.-H. Wang and Q. Shen, "Sonoluminescence tomography of turbid media," Opt. Lett. **23,** 561–563 (1998).
7. F. A. Marks, H. W. Tomlinson, and G. W. Brooksby, "Comprehensive approach to breast cancer detection using light: photon localization by ultrasound modulation and tissue characterization by spectral discrimination," in *Photon Migration and Imaging in Random Media and Tissue*, B. Chance and R. R. Alfano, eds., Proc. SPIE **1888,** 500–510 (1993).
8. L.-H. Wang, S. L. Jacques, and X. Zhao, "Continuous-wave ultrasonic modulation of scattered laser light to image objects in turbid media," Opt. Lett. **20,** 629–631 (1995).
9. L.-H. Wang and X. Zhao, "Ultrasound-modulated optical tomography of absorbing objects buried in dense tissue-simulating turbid media," Appl. Opt. **36,** 7277–7282 (1997).
10. M. Kempe, M. Larionov, D. Zaslavsky, and A. Z. Genack, "Acousto-optic tomography with multiple scattered light," J. Opt. Soc. Am. A **14,** 1151–1158 (1997).
11. S. Leveque, A. C. Boccara, M. Lebec, and H. Saint-Jalmes, "Ultrasonic tagging of photon paths in scattering media: parallel speckle modulation processing," Opt. Lett. **24,** 181–183 (1999).
12. G. Yao and L.-H. Wang, "Theoretical and experimental studies of ultrasound-modulated optical tomography in biological tissue," Appl. Opt. **39,** 659–664 (2000).
13. L.-H. Wang and G. Ku, "Frequency-swept ultrasound-modulated optical tomography of scattering media," Opt. Lett. **23,** 975–977 (1998).
14. G. Yao, S. Jiao, and L.-H. Wang, "Frequency-swept ultrasound-modulated optical tomography in biological tissue by use of parallel detection," Opt. Lett. **25,** 734–736 (2000).
15. J. Li, S. Sakadzic, G. Ku, and L.-H. Wang, "Transmission- and side-detection configurations in ultrasound-modulated optical tomography of thick biological tissues," Appl. Opt. **42,** 4088–4094 (2003).
16. J. Selb, L. Pottier, and A. C. Boccara, "Nonlinear effects in acousto-optic imaging," Opt. Lett. **27,** 918–920 (2002).
17. A. Lev and B. G. Sfez, "Direct, noninvasive detection of photon density in turbid media," Opt. Lett. **27,** 473–475 (2002).
18. L.-H. Wang, "Mechanisms of ultrasonic modulation of multiply scattered coherent light: an analytic model," Phys. Rev. Lett. **87,** 043903 (2001).
19. L.-H. Wang, "Mechanisms of ultrasonic modulation of multiply scattered coherent light: a Monte Carlo model," Opt. Lett. **26,** 1191–1193 (2001).
20. S. Sakadzic and L.-H. Wang, "Ultrasonic modulation of multiply scattered coherent light: an analytical model for anisotropically scattering media," Phys. Rev. E **66,** 026603 (2002).
21. W. Leutz and G. Maret, "Ultrasonic modulation of multiply scattered light," Physica B **204,** 14–19 (1995).
22. G. Marquez, L.-H. Wang, S.-P. Lin, J. A. Schwartz, and S. L. Thomsen, "Anisotropy in the absorption and scattering spectra of chicken breast tissue," Appl. Opt. **37,** 798–805 (1998).